

Floquet states of kicked particle in a singular potential: Exponential and power-law profile

Sanku Paul* and M. S. Santhanam†

Indian Institute of Science Education and Research, Dr. Homi Bhabha Road, Pune 411 008, India.

(Dated: February 26, 2019)

It is well known that, in the chaotic regime, all the floquet states of kicked rotor system display an exponential profile resulting from dynamical localization. If the kicked rotor is placed in an additional stationary infinite potential well, the floquet states of this non-KAM system are known to display power-law decay profile. It has also been suggested in general that in the case of periodically kicked systems with singularities in the potential, the floquet states would display power-law profile. In this work, we examine this question by studying the floquet states of a kicked particle in finite potential barriers. We map this system to a tight binding model and show that the occurrence of exponential or power-law profile of floquet states depends on the effective strength of singularity experienced by the floquet states in their energy band. Thus, the decay profile of the floquet state is a combination of both exponential and power-law profile depending on strength of singular potential. The signatures of this property can also be inferred from nearest neighbour spacing distribution as well in the statistics of eigenvectors. Quite unusually, this leads to a scenario in which the level spacing distribution, as a window in to the spectral correlations, is not a unique characteristic for the entire system.

I. INTRODUCTION

Quantum localization in chaotic systems continues to attract attention in a variety of contexts ranging from entanglement measures [1] to transport and decoherence effects [2–4]. Most of such studies have focussed on kicked rotor as a paradigmatic model for time-dependent potential exhibiting chaotic dynamics. For sufficiently strong non-linearity, kicked rotor displays chaotic dynamics associated with diffusive energy growth with time. In the corresponding quantum regime, this unbounded energy growth is strongly suppressed by localization arising from destructive quantum interferences [5]. This effect in kicked rotor has been shown to be analogous to Anderson localization [6–8]. One significant property shared by the quantum kicked rotor and Anderson model is the exponential decay of their eigenstates. In the one dimensional Anderson model all the eigenstates are exponentially localized in position representation [9, 10], i.e., $\psi(x) \sim e^{-x/x_l}$ where x_l is the localization length. In the kicked rotor system, eigenstates are localized in the momentum representation. The latter has been experimentally realized in microwave ionization of hydrogen atoms and in cold atomic cloud in optical lattices [11, 13].

Kicked rotor can thus be regarded as a representative dynamical system from two distinct points of view. Firstly, in the classical sense, it belongs to a class of chaotic systems that obeys Kolmogorov-Arnold-Moser theorem implying that as a chaos parameter is varied starting from its integrable limit, the quasi-periodic orbits are gradually destroyed and the system eventually makes a gradual transition to predominantly chaotic dynamics. Secondly, in the quantum mechanical regime,

kicked rotor is paradigmatic example of dynamical localization and the associated exponential profile of its eigenstates. In the last one decade, many other facets of chaos and localization in variants of kicked rotor have been studied that have provided results different from the standard scenario described above.

One class of important variant is to place the kicked rotor in additional singular potential. Presence of singularity in the potential violates one of the conditions for the applicability of KAM theorem and leads to a scenario in which abrupt transition from integrability to chaos becomes possible. This is a dynamical feature of non-KAM systems and is seen, for instance, in the kicked particle in an infinite potential well [14, 15]. The quantum eigenstates of this system has been briefly reported to display localization and its profile is *not* exponential but was claimed to have power-law type decay in the unperturbed basis. A more systematic study in Ref [16] incorporated singularity in the kicked rotor potential through a tunable logarithmic term. It was shown, through numerical simulations, that at the point of singularity in the potential all the eigenstates are power-law localized. Indeed, it was even suggested that kicked rotor when acted upon by a singular potential would display eigenstate localization with power-law profile in contrast to the exponential profile obtained in the context of standard KR [15, 17]. This suggestion has not yet been numerically tested in a variety of chaotic Hamiltonian systems and a general analytical support for this claim remains an open question.

In this paper, we examine the question if the presence of non-analytic potential and non-KAM type dynamics in a kicked rotor variant would imply powerlaw profile for its eigenstates in the quantum regime. To address this question, we consider the dynamics of a periodically kicked particle placed in a finite potential well. This is primarily a non-KAM system and its unusual classical and quantum transport properties, reflective of its non-

* Email: sankup005@gmail.com

† Email: santh@iiserpune.ac.in

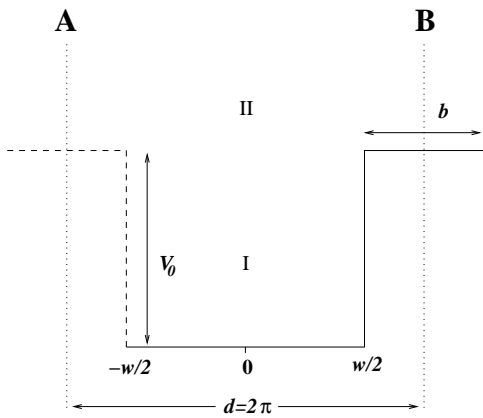


FIG. 1. Schematic of the stationary potential, $V_{sq}(\theta)$ with V_0 as the potential height, b and w as barrier and well width. A and B represents the positions at which periodic boundary conditions are applied. I and II denotes the regions below and above V_0 .

KAM nature, were recently reported [18]. This system subsumes two limiting cases; it is the standard kicked rotor (a KAM system) in the absence of finite well potential. When the finite well is taken as an infinite well, it becomes a non-KAM system studied in Refs [14, 15]. Hence, this is a suitable test bed to understand the quantum manifestations of non-KAM systems. As we show in this work using the context of this system, the spectral fluctuation properties, both of the eigenvalues and eigenvectors, strongly depend on the energy scales and is not homogeneous throughout the system. Such energy scale dependent spectral fluctuations are not usually seen in quantum chaotic systems.

II. KICKED PARTICLE IN FINITE BARRIER

The dimensionless Hamiltonian of a periodically kicked particle in a finite well potential [18] is

$$\begin{aligned} H &= \frac{p^2}{2} + V_{sq}(\theta) + k \cos(\theta) \sum_{n=-\infty}^{\infty} \delta(t - n) \\ &= H_0 + V(\theta) \sum_{n=-\infty}^{\infty} \delta(t - n). \end{aligned} \quad (1)$$

In this, $V(\theta) = k \cos(\theta)$ and $V_{sq}(\theta)$ is the square well potential shown in Fig. 1 and can be represented as

$$V_{sq}(\theta) = V_0[\Theta(\theta - R\pi) - \Theta(\theta - R\pi - b)]$$

where V_0 is the potential height and b is the barrier width, $R = w/\lambda$ is the ratio of well width to the wavelength of the kicking field and k is the kick strength. Throughout this work, we have set $\lambda = 2\pi$, b and w are constrained by $b + w = 2\pi$. Periodic boundary conditions are applied at positions A and B shown in Fig. 1.

Let E_n and $|\psi_n\rangle$ represent the energy and the eigenstate of the unperturbed system such that $H_0|\psi_n\rangle = E_n|\psi_n\rangle$. Further, $|\psi_n\rangle$ can be written as a superposition of all momentum states $|l\rangle$, i.e. $|\psi_n\rangle = \sum_l a_{nl}|l\rangle$, where a_{nl} represents the expansion coefficient. Then any general initial state can be expressed in the energy basis state representation as $|\Psi\rangle = \sum_n b_n|\psi_n\rangle$. The mean energy of the system in the state $|\Psi(t)\rangle$ can be obtained as

$$\begin{aligned} E(t) &= \langle \Psi(t) | \hat{H}_0 | \Psi(t) \rangle \\ &= \sum_m E_m |b_m(t)|^2 \end{aligned} \quad (2)$$

The quantum map that connects the state $|\Psi(N+1)\rangle$ at time $N+1$ with the state $|\Psi(N)\rangle$ can be obtained by evolving the Schrodinger equation $|\Psi(N+1)\rangle = \hat{U}|\Psi(N)\rangle$, where \hat{U} is the floquet operator,

$$\hat{U} = e^{-H_0 t/\hbar_s} e^{-iV(\theta)/\hbar_s} \quad (3)$$

and \hbar_s is the scaled Planck's constant. In the energy representation, the elements of the floquet operator are given by

$$U_{nm} = \sum_{p,p'} a_{np}^* a_{mp'} i^{|p-p'|} J_{|p-p'|} \left(\frac{k}{\hbar_s} \right), \quad (4)$$

where $J_{|p-p'|}(\cdot)$ is the Bessel function of order $|p-p'|$.

The eigenvalue equation governing the floquet operator is $\hat{U}|\phi\rangle = e^{i\omega}|\phi\rangle$ in which $|\phi\rangle$ represents a floquet state and ω is its quasi-energy. The floquet operator is an unitary operator and hence the eigenvalues lie on a unit circle. Further the quasi-energy state, $|\phi\rangle$, can be decomposed as a superposition of all energy states $|\psi_n\rangle$, i.e., $|\phi\rangle = \sum_n c_n|\psi_n\rangle$, where $|c_n|$ is the probability density of finding the particle in state $|\psi_n\rangle$.

In order to analyse the localization properties of the floquet states, floquet matrix of order N is numerically diagonalised to determine the quasi-energies and the floquet vectors. In this work, N is taken to be 10035 and all the parameters used in this paper, the system is classically chaotic. Floquet states for standard kicked rotor are generally known to be exponentially localized in momentum space $|\psi(p)|^2 \sim \exp(-p/\xi)$ characterised by a localisation length ξ . In contrast to that, floquet states of a particle in a periodic potential well is localized over energy basis state $|\psi\rangle$. And the system exhibits a smooth transition from exponential to power-law localisation by varying system parameters V_0 and k and is clearly shown in Fig 2.

III. FLOQUET STATES

In this section, we will mainly focus on the average spectral properties of the floquet states which governs

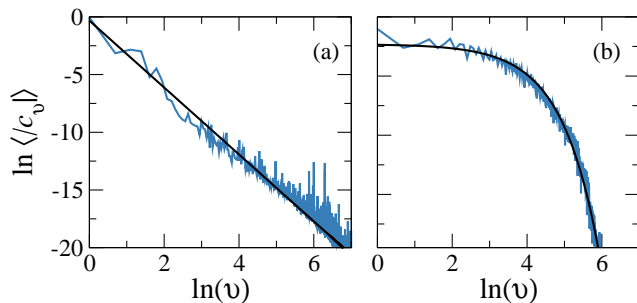


FIG. 2. Decay of floquet states over the unperturbed basis states, averaged over all the floquet states. The parameters are $b = 1.4\pi$, $\hbar_s = 1.0$, (a) (KRIW limit) $V_0 = 5000.5$, $k = 0.25$, and (b) (KR limit) $V_0 = 0.5$, $k = 4.25$. In (a) black line is a linear fit and in (b) black curve is an exponential fit.

the dynamics in the quantum regime. For the finite well represented by Hamiltonian in Eq. 1, the nature of floquet state decay profile, in general, will depend on the choice of parameters, namely, kick strength k and potential height V_0 . Fig. 2 has been obtained by averaging over 10035 floquet states $|\phi\rangle (= \sum_n c_n |\psi_n\rangle)$ for each set of parameters. Prior to averaging, each floquet state was shifted by n_{max} , where n_{max} corresponds to n for which $|c_n|^2$ is maximum.

If $V_0 > 0$, the Hamiltonian in Eq. 1 is a non-KAM system due to the presence of singularities in $V_{sq}(\theta)$. Based on numerical simulations of kicked systems with singular potentials, it was argued that their floquet states display power-law decay over the unperturbed basis [14–17, 19]. Further, a new universality class has been proposed in Ref. [16] based on the presence of classical singularity and power-law localization. To discuss the results, in the light of this proposal, two limiting cases can be identified; (i) $0 < V_0 < 1$ (kicked rotor (KR) limit) and (ii) $V_0 \gg 1$ (kicked rotor in infinite well (KRIW) limit). In the KR limit, notwithstanding the singularity in the potential, the floquet states can be expected to be qualitatively closer to that of kicked rotor. In particular, if kick strength $k \gg 1$, all the floquet states display exponential decay profile. On the other hand, in the KRIW limit, the potential height is large ($V_0 \gg 1$) and is qualitatively closer to the kicked infinite well system [14, 15]. In this limit, even for small kick strengths $k < 1$, it is known that all the floquet states show power-law decay over the unperturbed basis [15, 17]. Both these limits are illustrated in Fig. 2.

In Fig. 2(a), the decay of the averaged floquet state in the KRIW limit is shown for $V_0 = 5000.5$ and $k = 0.25$. It is consistent with a power-law form $P(v) \sim v^{-\gamma}$, where $v = n - n_{max} > 0$ and $\gamma \approx 2.5$, in agreement with the value reported in Ref. [15] and the deviation observed can be attributed to the finite height of well. On the other hand, averaged floquet state in the KR limit for $V_0 = 0.5$ and $k = 4.25$ displays exponential decay, $P(v) \sim \exp(-v/l)$, where l is the localization length. This is the standard dynamical localization scenario but

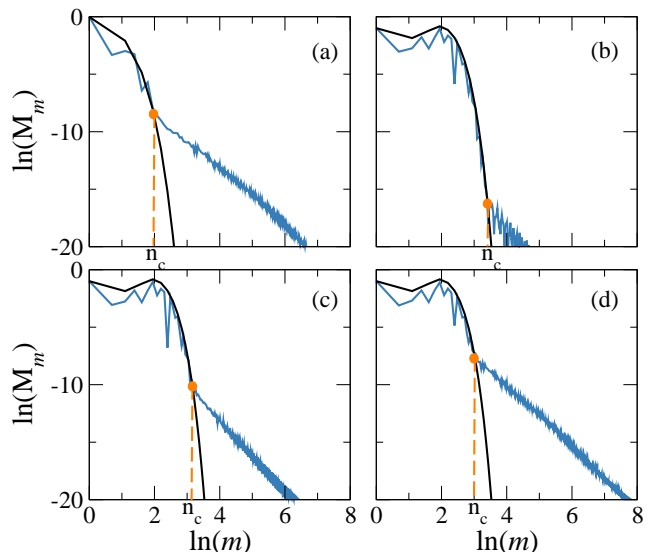


FIG. 3. Averaged decay of the matrix elements of the Floquet operator \hat{U} as a function of m . The parameters are $b = 1.4\pi$, $\hbar_s = 1.0$, (a) (KRIW limit) $V_0 = 5000.5$, $k = 0.25$, and (b) (KR limit) $V_0 = 0.5$, $k = 4.25$, (c) $V_0 = 100.0$, $k = 4.25$, (d) $V_0 = 5000.5$, $k = 4.25$. All black curves corresponds to KR.

is generally not associated with non-KAM systems. Both these decay profiles in Fig. 2 can be understood if the relation between singular potential and power-law localization can be restated in the following manner. For this purpose, let $\Delta\epsilon_f$ represents a energy band in the unperturbed basis. The classical singularities are associated with quantum power-law localization of a set of floquet states mostly lying in the energy range $\Delta\epsilon_f$, provided $\Delta\epsilon_f < V_0$. Effectively, floquet states will display power-law localization only if they effectively “feel” the non-smooth potential. This requires that energy scale $\Delta\epsilon_f$ must be less than that representing the potential height.

It must be emphasised that the Hamiltonian in Eq. 1 is classically a non-KAM system if $V_0 > 0$, for all values of $k > 0$. Hence, with $V_0 = 5000.5$ and for kick strength as small as $k = 0.25$ the system is classically chaotic and the corresponding quantized system displays power-law localized profile of the floquet states (Fig. 2(a)). In this case, most of the 10035 floquet states used for averaging and shown in Fig. 2(a) are such that $\Delta\epsilon_f < V_0$. On the other hand, in the case of Fig. 2(b), even though it is still a non-KAM system with singular potential, the floquet states mostly straddle energy scales larger than $V_0 < \Delta\epsilon_f$. and are not affected by the shallow singular potential and hence the exponentially localized floquet states.

A. Matrix element decay

It is known that exponential localization in the kicked rotor is associated with the exponential decay of the ma-

trix elements of the corresponding Floquet operator. Further, from Ref. [14, 15], it is also known that in the case of kicked rotor in the infinite well, a non-KAM system, the matrix elements of \hat{U} display a power-law decay after a bandwidth $\eta \propto k$. Hence, it is natural to enquire how the decay of matrix elements changes its character as $V_0 \gg 1$ approaches the limit $V_0 \rightarrow 0$. In the unperturbed basis, the matrix elements are U_{nm} as given by Eq. 4. This is illustrated in Fig. 3 which shows $M_m = \langle |U_{nm}| \rangle_n$ as a function of m , with $m > n$, in log-log plot.

Figure 3(a,b) shows M_n as log-log plot for the same choice of parameters as in Fig. 2(a,b). Figure 3(a) corresponds to KRIW limit and shows a short regime of exponential decay followed by an asymptotic power-law decay. In Fig. 3(b), $V_0 = 0.5$ corresponding to the KR limit and the decay of M_n largely follows that of KR except for $n \gg 1$ where it decays as a power-law. In general, the following features are observed. In the limit as $V_0 \rightarrow \infty$, the decay is of power-law form. In the opposite limit of $V_0 \rightarrow 0$, the decay is exponential in nature. In general, for any intermediate V_0 , i.e., $0 < V_0 < \infty$, an initial exponential decay is followed by an asymptotic power-law decay whose slope is approximately 2.7. If $V_0 < \infty$, the initial exponential decay is always present. Let the exponential decay sharply change over to a power-law decay at $n = n_c$ as shown by dotted vertical lines in Fig. 3. For any fixed value of kick strength k , as V_0 varies from $0 \rightarrow \infty$, then n_c changes from $\infty \rightarrow 0$. It is also to be noted that for fixed V_0 , as k increases, n_c tends towards larger values.

B. Energy scales

In this section, we show how singularity of the potential and energy scales associated with the Floquet states determine the localization structure of these states. As discussed in sec. 2, $c_{rj} = \langle \phi_r | \psi_j \rangle$ where $|\psi_j\rangle$ is an eigenstate of H_0 with associated energy E_j . Let $c_{max} = \max(|c_{r,1}|^2, |c_{r,2}|^2, \dots, |c_{r,N}|^2)$ represent the largest overlap of r -th Floquet state with $|\psi_j\rangle$. The energy associated with $|\psi_j\rangle$, and hence with c_{max} , is denoted by E_{max} . Then, an effective parameter $\mu = E_{max}/V_0$ can be identified to distinguish two regimes, namely, (i) $\mu \leq 1$ and (ii) $\mu \gg 1$. Physically, $\mu \leq 1$ corresponds to Floquet states (in energy basis) mostly confined to the potential height V_0 and $\mu \gg 1$ corresponds to those Floquet states that have significant overlap with states lying in the energy scales far greater than V_0 .

In Fig. 4(a), $\ln\langle c_v \rangle$ is shown by averaging over all the computed Floquet states for $V_0 = 5000.5$ and $k = 4.25$. As discussed earlier, the Floquet state profile is a combination of initial exponential decay followed by a power-law decay. However, if average is taken only over those states that satisfy the condition $\mu \leq 1$, then the resulting profile is shown in Fig. 4(b). In this case $k = 4.25$ and all the Floquet states are confined to an energy

scale well below V_0 . Hence, these set of Floquet states can be expected to “feel” the presence of singularity in the potential. In this regime, we observe a power-law profile for the averaged Floquet states in Fig. 4(b).

However if the states are averaged subject to the condition that $\mu \gg 1$, then singularity is not strongly felt by the Floquet states since the bandwidth of their energy distribution is far greater than V_0 . Effectively, at this energy scale, the singularity becomes insignificant and hence we can expect it to lie in the KR limit. Indeed, as seen in Fig. 4(c), $\langle c_v \rangle$ is nearly identical to that of kicked rotor (shown as black curve in Fig. 4(c)) at $k = 4.25$.

In general, for the Hamiltonian in Eq. 1, the localization property of a subset of Floquet states in an energy band $\Delta\epsilon_f$ depends on the effectiveness of the singularity for the spectral range $\Delta\epsilon_f$ under consideration. In a given energy band $\Delta\epsilon_f$, if the singularity is effective, then power-law localization is obtained and if singularity is weak or absent then exponential localization results for the states in $\Delta\epsilon_f$. As far as localization of eigenstates of chaotic systems are concerned, it is known that either all the states are exponentially localized (as in kicked rotor) or power-law localized (as in systems with singular potentials) but, to the best of our knowledge, combinations of these localization profiles have not been reported before. In the next section, we transform the Hamiltonian in Eq. 1 to that of a tight binding model and show that V_0/E controls the localization property of eigenvectors.

IV. TIGHT BINDING MODEL

The dynamical localization in the quantum kicked rotor system was mapped to Anderson model for electron transport in a one-dimensional crystalline lattice [6]. By implication, the exponential decay profile of eigenstates in the Anderson model translates to exponential profile (in the momentum representation) for the Floquet states of quantum kicked rotor. Following this mapping technique, in this section, we map the Hamiltonian in Eq. 1 to a tight binding Hamiltonian. Since Eq. 1 represents a time periodic system, using Floquet-Bloch theorem, we can write the quasienergy state as

$$\phi(\theta, t) = e^{-i\omega t} u(\theta, t) \quad (5)$$

where, $u(\theta, t) = u(\theta, t + 1)$. In between two consecutive kicks, the Hamiltonian H_0 governs the evolution of the particle and is given by,

$$\phi_n^-(t + 1) = e^{-iE_n} \phi_n^+(t). \quad (6)$$

In this, $\phi_n^-(t + 1)$ and $\phi_n^+(t)$ are the quasienergy states just before the $(t + 1)$ -th kick and just after t -th kick and E_n is the n -th energy level of H_0 . During the evolution it acquires an extra phase e^{-iE_n} . By substituting Eq. 5 in Eq. 6 and using the periodicity of $u(\theta, t)$, we obtain

$$u_n^-(\theta, t + 1) = e^{i\omega} e^{-iE_n} u_n^+(\theta, t) \quad (7)$$

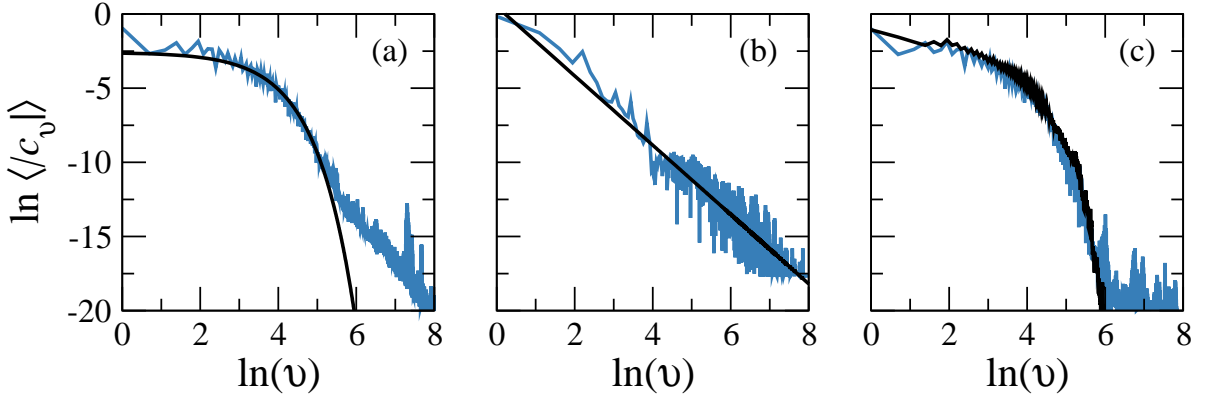


FIG. 4. Floquet states of Hamiltonian in Eq. 1 with parameters $b = 1.4\pi$, $\hbar_s = 1.0$, $V_0 = 5000.5$, $k = 4.25$. The three figures differ in how floquet states were averaged over; (a) averaged over all the computed states, (b) averaged over states with $\mu < 1$, (c) averaged over states with $\mu \gg 1$. In (a,b) black curve represent best fit line and in (c) black curve corresponds to KR.

Now the quasienergy state just after a t -th kick can be obtained using a map $\phi^+(\theta, t) = e^{-iV(\theta)}\phi^-(\theta, t)$. By using Eq. 5, this can be written in-terms of $u(\theta, t)$ as

$$u^+(\theta, t) = e^{-iV(\theta)}u^-(\theta, t) \quad (8)$$

Now, $e^{-iV(\theta)}$ is expressed in terms of trigonometric function $W(\theta) = -\tan\left(\frac{V(\theta)}{2}\right)$ as

$$e^{-iV(\theta)} = \frac{1 + iW(\theta)}{1 - iW(\theta)}. \quad (9)$$

This is used in Eq. 8 to obtain

$$\frac{u^+(\theta)}{1 + iW(\theta)} = \bar{u} = \frac{u^-(\theta)}{1 - iW(\theta)} \quad (10)$$

where \bar{u} is defined as $\bar{u} = [u^+(\theta) + u^-(\theta)]/2$. Using Eq. 8,9, the evolution of the quasienergy state after one period is

$$u^+(\theta) = e^{-iV(\theta)}e^{i(\omega - E_n)}u^+(\theta). \quad (11)$$

This can be written as,

$$(1 - iW(\theta))\bar{u} = e^{i(\omega - H_0)}\bar{u}(1 + iW(\theta)), \quad (12)$$

where $\bar{u} = \frac{u^+}{1 + iW(\theta)}$. Now rearrangement of terms leads to

$$\tan\left(\frac{\omega - H_0}{2}\right)\bar{u} + W(\theta)\bar{u} = 0. \quad (13)$$

Quasienergy state can be expanded in the unperturbed basis as $|\bar{u}\rangle = \sum_m u_m |\psi_m\rangle$ where, $|\psi_m\rangle$ are the eigenstates of H_0 and u_m is given by,

$$u_m = \int \bar{u}\psi_m(\theta)d\theta = \int \frac{1}{2}[u^+(\theta) + u^-(\theta)]\psi_m(\theta) d\theta. \quad (14)$$

Taking the inner product of Eq. 13 with $|\psi_m\rangle$, we will formally obtain

$$T_m u_m + \sum_l W_{ml} u_l = 0. \quad (15)$$

In this, $T_m = \tan\left(\frac{\omega - E_m}{2}\right)$ represents the on-site energy and W_{ml} is the hopping strength to hop a particle from m th site to l th site and can be written in the energy basis as

$$\begin{aligned} W_{ml} &= \langle \psi_m | W(\theta) | \psi_l \rangle \\ &= \int \sum_{p,q} a_{mp}^* e^{-ip\theta} W(\theta) a_{lq} e^{iq\theta} d\theta \\ &= \sum_{p,q} a_{mp}^* a_{lq} \int W(\theta) e^{-i(p-q)\theta} d\theta \\ &= \sum_{p,q} a_{mp}^* a_{lq} W_{p-q} \end{aligned} \quad (16)$$

where $W_n = \frac{1}{2\pi} \int_0^{2\pi} W(\theta) e^{-in\theta} d\theta$ is the Fourier transform of $W(\theta)$. Thus, in energy basis, after simple manipulation, Eq. 15 takes the form

$$\left(T_m + \sum_{p,q} a_{mp}^* a_{mq} W_{p-q} \right) u_m + \sum_{p,q,l \neq m} a_{mp}^* a_{lq} W_{p-q} u_l = 0. \quad (17)$$

This is the tight binding model version of the Hamiltonian in Eq. 1. In this, $(T_m + \sum_{p,q} a_{mp}^* a_{mq} W_{p-q})$ represents the diagonal term and $a_{mp}^* a_{lq} W_{p-q}$ is the off-diagonal term of the transfer matrix. It does not appear straightforward to analytically prove power-law profile of floquet states starting from Eq. 17, though it appears fair to expect that in this case the decay of floquet state profile will be different from exponential form. As numerical results show, we obtain power-law localization. Similar results has also been reported in [20].

However, using Eq. 17, it is possible infer about floquet state profile in the limit $\mu \gg 1$. In this case $E_n \gg V_0$

and the singularity in the potential becomes insignificant. Effectively, the system behaves as a free particle with energy $E_n = \frac{\hbar_s^2 n^2}{2}$ and the wavefunction of H_0 is just the momentum eigenstate,

$|\psi_n\rangle = a_{nn}e^{in\theta}$, with $a_{mn} = \delta_{mn}$. This set of conditions, if applied to Eq. 17, lead to

$$(T_m + W_0)u_m + \sum_l W_{m-l}u_l = 0. \quad (18)$$

This is just standard kicked rotor transformed to the 1D Anderson model [6], for which all the eigenstates are known to display exponential profile. Hence, as seen in Fig. 4(c) for $\mu \gg 1$, the observed localisation is exponential in nature. Thus, even in the presence of singular potentials, eigenstate localization is not generically of power-law form. We reiterate the main result of the paper that the association between power-law profile of eigenstates and singular potentials needs to take into account the effectiveness of singularity in a given energy band.

V. SPECTRAL SIGNATURES

Based on the results presented in Fig. 4, a novel scenario for the spectral signatures can be expected. As the regimes $\mu < 1$ and $\mu \gg 1$ are traversed, by considering floquet states in a suitable energy band $\Delta\epsilon_f$, the decay profile of floquet state changes from power-law to exponential form. This would also imply that a unique spectral signature for the nearest neighbour spacing distribution $P(s)$, such as either the Poisson or Wigner, may not exist for the system as a whole. Quite unusually, $P(s)$ would depend on the energy band $\Delta\epsilon_f$ being considered. Thus, in the same system for a given choice of parameters, in the limit $\mu \gg 1$ (KR limit) we expect Poisson distribution and in the limit $\mu < 1$ (KRIW limit) we expect $P(s)$ to be closer to Wigner distribution or possibly, a Brody distribution.

The floquet operator \hat{U} being a unitary operator, all the eigenvalues are on a unit circle, $\omega_i \in [0, 2\pi)$. In this case, level density is constant ($\frac{N}{2\pi}$) and hence the unfolding of floquet levels is not necessary. To compute the spacing distribution, we have treated the eigenvalues of even and odd parity states separately. The nearest neighbour spacing distribution reveals two different forms; for $\mu < 1$ level repulsion is observed in the form of Brody distribution and for $\mu \gg 1$ level clustering is seen in the form of Poisson distribution. The regime of $\mu < 1$ corresponds to KRIW limit and power-law decay of floquet states (see Fig. 4(b)) and is associated with level correlations that are intermediate between uncorrelatedness and random matrix type level repulsion. On the other hand, the limit of $\mu \gg 1$ is KR limit and levels remain uncorrelated due to occurrence of dynamical localization. It must be emphasised that two different level spacing distributions and level correlations for the same system

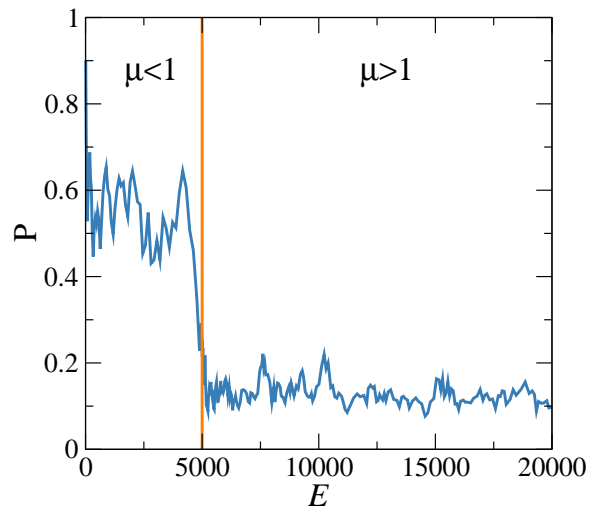


FIG. 5. Participation ratio of the floquet states as a function of E_{max} for $b = 1.4\pi$, $\hbar_s = 1.0$, $V_0 = 5000.5$, $k = 4.25$ (same set of parameters as in Fig. 4). The vertical line is placed at $E_{max} = V_0$ ($\mu = 1$), the height of potential barriers.

with identical parameters is a novel feature not usually encountered in the context of chaotic quantum systems. This unusual spacing distribution reinforces the central result of this paper that the relation between potential singularity and eigenvector profile is conditioned by energy regime being considered.

This dichotomy is reflected in the eigenvector statistics as well. This is easily observed by studying the participation ratio (PR) of the floquet states that provides information about their localization properties. For an eigenstates that resides in the infinite dimensional Hilbert space, participation ratio is defined as

$$P = \sum_{i=1}^{\infty} |\psi_i|^4 \quad (19)$$

with the condition that $\sum_i |\psi_i|^2 = 1.0$, where ψ_i are components of a floquet state. It is a measure of how many basis states effectively participate in making up the eigenstate. If $P \approx 1$, then the state is strongly localized and implies that one basis state contributes significantly to the floquet state while the contribution from the rest of the basis are almost negligible. However, if $P \sim \frac{1}{N}$, then the floquet state is of extended nature and all the basis states make equal contribution on an average. Figure 5 displays P for all the 10035 converged floquet states as a function of energy E_{max} for the identical choice of parameters as in Fig. 4. Quite surprisingly, P distinguishes the two regimes, $\mu < 1$ and $\mu \gg 1$. The boundary between the two regimes is at $E_{max} = V_0$, the height of potential barriers. For $\mu \gg 1$, exponential localisation of floquet states implies that $|\phi\rangle \sim e^{-n/l}$, where l is the localization length. A remarkable result due to Izrailev [5, 21] provides the relation, $l \approx \frac{k^2}{2\hbar_s^2}$. For our case, this estimate gives $l \approx \frac{k^2}{2\hbar_s^2} = 9.03$ and this represents the ef-

fective number of basis states that goes into constructing the floquet states. As participation ratio is the inverse of the effective number of basis states, it is estimated to be $P \approx \frac{2\hbar^2}{k^2} = 0.11$. As seen in Fig. 5, this value closely matches the computed PR in the regime $\mu \gg 1$.

For $\mu < 1$, the mean P is larger compared to that for $\mu > 1$ as shown in Fig. 5. The reason can be traced back to the fact that in the case of infinite well $E_n \sim n^2$ and hence levels are spaced far apart. This implies that the floquet states for $\mu < 1$ has overlap only with a few unperturbed basis states and this effectively increases the value of participation ratio for $\mu < 1$. Ultimately, this results in a more compact localisation.

VI. CONCLUSION

In summary, we have studied a non-KAM system represented by the Hamiltonian in Eq. 1, namely a periodically kicked particle in a finite potential well of height V_0 , to primarily understand the nature of its floquet states. This Hamiltonian can be thought of as representing two limiting cases, (i) the standard kicked rotor for $V_0 = 0$ and (ii) kicked rotor in infinite potential well for $V_0 \rightarrow \infty$. It is well known that, for sufficiently large kick strengths, all the floquet states of the kicked rotor are localized with an exponential profile [5]. Further, it has been suggested that for kicked systems with singularity in their potential, the floquet states display power-law profile [17]. We examine the floquet states of the Hamiltonian in Eq. 1 in the light of these results. To understand its floquet states, we map this problem to that of a tight binding model.

The results presented in this work show that the decay profile of the floquet states is not determined by the potential singularity alone, but by the representative energy band $\Delta\epsilon_f$ of a set of floquet states relative to the potential height V_0 . Thus, we show that if $\Delta\epsilon_f > V_0$ then the effect of singularity is weak for those set of floquet states and they display exponential profile. This represents the kicked rotor limit of the problem. On the other hand, the condition $V_0 > \Delta\epsilon_f$ represents floquet states strongly affected by the singular potential. In this case, we have shown that floquet states have predominantly power-law profile. In the region intermediate between these two extremes, the floquet states typically display an initial exponential decay followed by an asymptotic power-law decay. The presence of these two contrasting floquet state profiles in Hamiltonian in Eq. 1 leaves its signature in the spectral correlations as well. For identically same set of parameters, depending on the reference energy scale $\Delta\epsilon_f$, the spacing distribution turns out to be Poisson distribution ($\Delta\epsilon_f > V_0$) or a general Brody distribution ($V_0 > \Delta\epsilon_f$). Typically, the spacing distribution is taken to characterise quantum chaos in a system and it is generally independent of the energy band being considered provided it is in the semiclassical limit. Quite surprisingly, the semiclassical limit of the system in Eq. 1 lacks a unique spacing distribution as it depends on the energy band $\Delta\epsilon_f$ being considered. Kicked rotor was experimentally realized in a test-bed of cold atomic cloud in flashing optical lattices. Using more than one optical lattice, kicked rotor confined to a ‘potential well’ has also been realized. We believe that the results in this work is amenable to experiments in a suitable atom-optics set up.

-
- [1] M. S. Santhanam, V. B. Sheorey, and Arul Lakshminarayanan, Phys. Rev. E **77**, 026213 (2008).
 - [2] S. Sarkar et. al., Phys. Rev. Lett. **118**, 174101 (2017); B. G. Klappauf, W. H. Oskay, D. A. Steck, and M. G. Raizen, Phys. Rev. Lett. **81**, 1203 (1998).
 - [3] W. H. Zurek, Rev. Mod. Phys. **75**, 715 (2003).
 - [4] H. Schomerus and E. Lutz, Phys. Rev. Lett. **98**, 260401 (2007); Phys. Rev. A **77**, 062113 (2008).
 - [5] F. M. Izrailev, Phys. Rep. **196**, 299 (1990).
 - [6] S. Fishman, D. R. Grempel, and R. E. Prange, Phys. Rev. Lett. **49**, 509 (1982); D. R. Grempel, R. E. Prange and S. Fishman, Phys. Rev. A **29**, 1639 (1984).
 - [7] H-J. Stockmann, *Quantum Chaos: An Introduction* (Cambridge University Press, Cambridge, 1999).
 - [8] L. Reichl, *The Transition to chaos : Conservative classical systems and quantum manifestations*, (Springer, 2004).
 - [9] P. W. Anderson, Phys. Rev. **109**, 1492 (1958).
 - [10] 50 Years of Anderson Localization, edited by E. Abrahams (World Scientific, Singapore, 2010).
 - [11] F. L. Moore, J. C. Robinson, C. F. Bharucha, Bala Sundaram, and M. G. Raizen, Phys. Rev. Lett. **75**, 4598 (1995).
 - [12] J. Ringot, P. Szriftgiser, J. C. Garreau, and D. Delande, Phys. Rev. Lett. **85**, 2741 (2000).
 - [13] T M Fromhold et. al., J. Opt. B: Quantum Semiclass. Opt. **2**, 628 (2000).
 - [14] R. Sankaranarayanan, A. Lakshminarayanan, V.B. Sheorey, Phys. Rev. E **64**, 046210 (2001).
 - [15] B. Hu, B. Li, J. Liu, and Y. Gu, Phys. Rev. Lett. **82**, 4224 (1999).
 - [16] A. M. Garcia-Garca and J. Wang, Phys. Rev. Lett. **94**, 244102 (2005)
 - [17] J. Liu, W. T. Cheng, and C. G. Cheng, Commun. Theor. Phys. **33**, 15 (2000).
 - [18] S. Paul, H. Pal, and M. S. Santhanam, Phys. Rev. E **93**, 060203(R) (2016); H. Pal and M. S. Santhanam, Phys. Rev. E **82**, 056212 (2010).
 - [19] J. V. Jose and R. Cordery, Phys. Rev. Lett. **56**, 290 (1986).
 - [20] A. Cohen and S. Fishman, Int. J. Mod. Phys. B **02**, 103 (1988).
 - [21] B. V. Chirikov, F. M. Izrailev, and D. L. Shepelyansky, Sov. Sci. Rev. **2C**, 209 (1981).